



ELSEVIER

Journal of Chromatography A, 910 (2001) 51–60

---

---

JOURNAL OF  
CHROMATOGRAPHY A

---

---

www.elsevier.com/locate/chroma

# Characterization of polystyrene and polyisoprene by normal-phase temperature gradient interaction chromatography

Wonmok Lee, Donghyun Cho, Byung Ok Chun, Taihyun Chang\*, Moonhor Ree

*Department of Chemistry and Center for Integrated Molecular Systems, Pohang University of Science and Technology, Pohang 790-784, South Korea*

Received 28 June 2000; received in revised form 6 November 2000; accepted 10 November 2000

---

## Abstract

Temperature gradient interaction chromatography (TGIC) is applied to the characterization of polyisoprene (PI) and polystyrene (PS) using normal-phase (NP) stationary phase – bare silica or diol bonded silica. Tetrahydrofuran–isooctane mixtures are used as a mobile phase. PI and linear and star shaped PS samples are successfully fractionated in terms of the molecular mass with a high resolution comparable to that of reversed-phase (RP) HPLC. Temperature dependence of the retention shows that the enthalpy of adsorption of PS to the stationary phase is exothermic. In addition, some characteristic features of the NP-TGIC system relative to those of RP-TGIC are presented, which include a high sensitivity on the polar end group and the simultaneous size-exclusion chromatographic and TGIC characterization of PS and PI mixtures. © 2001 Elsevier Science B.V. All rights reserved.

*Keywords:* Temperature gradient interaction chromatography; Polymers; Polystyrene; Polyisoprene

---

## 1. Introduction

By virtue of the recent development of liquid chromatography (LC), there has been significant progress on the fractionation of macromolecules. Among numerous variations of LC methods, size-exclusion chromatography (SEC) has been the most popular method for the characterization of molecular mass distribution (MWD) of synthetic and natural polymers [1–3]. Nevertheless, since SEC separates the polymer molecules according to their size only, it is not an efficient method to separate polymers in terms of chemical heterogeneity, such as chemical

composition difference of copolymers, tacticity, and end-group difference. Furthermore, the resolution of SEC is limited due to the band broadening effect and it is often impossible to characterize the accurate MWD of polymers with narrow MWD such as most anionically polymerized polymers [4].

For a couple of decades, reversed-phase liquid chromatography (RPLC) has been applied for the fractionation of high-molecular-mass polymers [5–16]. RPLC exhibits a much higher resolution than SEC. Recently, Chang and co-workers have reported successful applications of the temperature gradient RPLC in the molecular mass distribution analysis of various polymers such as polystyrene (PS) [17–21], polyisoprene (PI) [22] and poly(methyl methacrylate) (PMMA) [23]. In the separation technique named temperature gradient interaction chromatography

---

\*Corresponding author. Tel.: +82-54-2792-109; fax: +82-54-2793-399.

*E-mail address:* tc@postech.ac.kr (T. Chang).

(TGIC), the column temperature is varied during the elution in a pre-programmed manner to control the retention of polymeric solutes. TGIC was applied to the analysis of MWD analysis not only for linear high-molecular-mass polymers but also for oligomers [20,22], star shaped PS [18,19] and polymer mixtures [24,25]. All of these studies were performed using alkyl chain bonded reversed-phase (RP) stationary phase. Although the majority of recent LC studies on the characterization of polymers employs RP mode, normal-phase liquid chromatography (NPLC) has a longer history than RPLC and has been frequently applied to the analysis of various oligomers and polymers [2,26–36]. Despite the many applications of NPLC to polymer analysis, we found that little efforts have been devoted to rigorous MWD characterization of high-molecular-mass polymers using NPLC. The resolution of NPLC was reported poorer than RPLC, particularly for high-molecular-mass polymers [6]. In this study, we applied NP-TGIC to characterize MWD of anionically synthesized polymers and compared the results with those of RP-TGIC. Since NPLC can be used more efficiently than RPLC for the fractionation according to the polar groups present in the polymers, we tested NP-TGIC for the polar end group

selectivity using high-molecular-mass PSs with different end groups.

## 2. Experimental

PS and PI samples were first characterized by SEC with two mixed bed columns (Polymer Lab. Mixed-C, 300 mm×8 mm I.D.). Chromatograms were recorded with a multi-angle light scattering detector (Wyatt, mini-DAWN) and a refractive index detector (Wyatt, Opti-Lab) using tetrahydrofuran (THF; Aldrich, HPLC grade) as a mobile phase. Injection samples were dissolved in THF at an appropriate concentration (0.05~2 mg/ml depending on the molecular mass) for light scattering detection and injected through a six-port sample injector (Rheodyne, 7125) equipped with a 50- $\mu$ l sample loop. The flow-rate of the mobile phase was 0.8 ml/min. Column temperature was kept at 40°C during the SEC run using a column oven (Eppendorf, TC-50). Chromatograms were collected and processed by Astra software. Calculated MWD data are summarized in Table 1. All the PI samples were prepared by anionic polymerization in cyclohexane solvent at 45°C under an Ar atmosphere using 2-butyl lithium

Table 1  
Characterization of the polymers used in this study

Sample code	$M_w$ ( $\cdot 10^3$ )		$M_w/M_n$		Microstructure of PI <sup>b</sup> (1,4- <i>trans</i> :1,4- <i>cis</i> :vinyl)	Sample source
	SEC-LS <sup>c</sup>	NP-TGIC	SEC-LS <sup>c</sup>	NP-TGIC		
PI-1	2.7 <sup>a</sup>		1.08		27:66:7	Laboratory made
PI-2	11.9 <sup>a</sup>		1.02		25:69:6	Laboratory made
PI-3	20.0		1.01		20:74:6	Laboratory made
PI-4	53.0	51.8	1.01	1.015	20:75:5	Laboratory made
PI-5	96.0	99.5	1.01	1.005	23:71:6	Laboratory made
PI-6	148	153.1	1.03	1.004	25:69:6	Laboratory made
PI-7	208		1.06		23:71:6	Laboratory made
PS-1	10.3		1.03			Laboratory made
PS-2	32.7		1.02			Laboratory made
PS-3	68.1	68.1	1.02	1.006		Laboratory made
PS-4	112	112.3	1.02	1.005		Laboratory made
PS-5	213	205.7	1.02	1.004		Pressure chemical
PS-6	394	395.5	1.02	1.003		Waters
PS-7	683	653.4	1.03	1.006		Laboratory made
PS-8	1530		1.03			Daelim

<sup>a</sup> Calculated by universal calibration to PS standards.

<sup>b</sup> Determined by <sup>1</sup>H-NMR.

<sup>c</sup> Light scattering detection.

as an initiator [37]. Therefore the microstructures of the PI samples are practically identical. In Table 1, the microstructure of PI samples characterized by 300 MHz  $^1\text{H}$ -nuclear magnetic resonance (NMR) (Bruker, DPX-300) are summarized. Laboratory-made PS samples were also prepared by the same method.

The NP-TGIC system is essentially the same as that of RP-TGIC system except for the column and the mobile phase [24]. It consists of a high-performance liquid chromatography (HPLC) pump (LDC, CM 3200), a six-port sample injector (Rheodyne, 7125), and a variable-wavelength UV–Vis absorption detector (TSP, SC-100) as a concentration detector. Mobile phase was a mixture of THF–isooctane (Aldrich, HPLC grade) of which the composition was adjusted to obtain a good separation efficiency for each polymer species studied. A silica column (Nucleosil, 100 Å, 250 mm×2.1 mm I.D.) was used for the TGIC analysis of PS while a diol bonded silica column (Nucleosil, 100 Å, 250 mm×2.1 mm I.D.) was used for PI. Polymer samples dissolved in the corresponding mobile phase (1.0 mg/ml) were injected and the peak absorbance of the UV–Vis detector signal was in the range of 0.02–0.05. The flow-rate of the mobile phase was 0.1 ml/min except for the simultaneous SEC–TGIC experiment in which three columns with 4.6 mm I.D. were used. The temperature of the separation column was controlled during the TGIC elution by circulating fluid from a programmable bath/circulator (NESLAB, RTE-111) through a laboratory-made column jacket. For simultaneous SEC–TGIC analysis of the PS–PI mixture, three silica columns with different pore sizes (Nucleosil, 100, 500, 1000 Å, respectively, 250 mm×4.6 mm I.D.) were connected and the flow-rate was 0.5 ml/min. For MWD calculation, a calibration curve was constructed by fitting the peak positions of corresponding standard samples to a polynomial.

### 3. Results and discussion

#### 3.1. Fractionation of PI

In order to achieve a good resolution of the TGIC separation for a polymer species, a set of a stationary

and an isocratic mobile phase has to be carefully chosen [23]. Recently, Czichocki et al. reported that the critical adsorption point (CAP) of PI could be established using bare silica and isooctane–THF mixture (0.88%, v/v, of THF) as a stationary and a mobile phase, respectively [34]. The TGIC separation condition is in general similar to the CAP condition [24] and the combination was tested first. It was possible to obtain a good TGIC resolution for PI with the CAP condition, however, it did not provide a good reproducibility in the retention. This is thought to be due to the sensitive variation of adsorbed THF amounts on the silica surface with the temperature change and the slow equilibration process [38]. In TGIC experiments, temperature is changed during the elution. The THF adsorption seems to change with temperature and it was necessary to re-equilibrate the column for every run to acquire satisfactory reproducibility. In order to have a good reproducibility, we needed to have the mixed eluent flow through the bare silica column for longer than 12 h. This time consuming step is in part due to the small content of THF (less than 1%) in the mixture. If we use a higher THF content eluent as in the PS fractionation detailed later, the pre-equilibrium run was not necessary. Therefore, for PI fractionation, we tried bonded stationary phase instead of bare silica since the homogeneity of the surface interaction with either solute or solvent was reported better in the bonded phase [39]. We tested CN bonded silica and diol bonded silica columns and found the latter provided better separation efficiency.

We found that mixtures of isooctane–THF worked well for NP-TGIC analysis of both PI and PS. Composition of THF was adjusted according to the polarity of each polymer system. For PI, a typical nonpolar polymer, 1.5% (v/v) THF worked well with a diol bonded stationary phase. In Fig. 1, NP-TGIC chromatograms of five anionically polymerized PI samples are shown. The temperature gradient program is also drawn at the right ordinate. For MWD analysis, PIs 4, 5, 6 were independently injected and the chromatograms are shown with dotted lines in the figure. Using a third-order polynomial function, peak positions of five PI samples were fitted to obtain a calibration curve ( $M$  vs.  $V_R$ ) for MWD analysis. The results are summarized in Table 1. The weight average molecular masses ( $M_w$ )

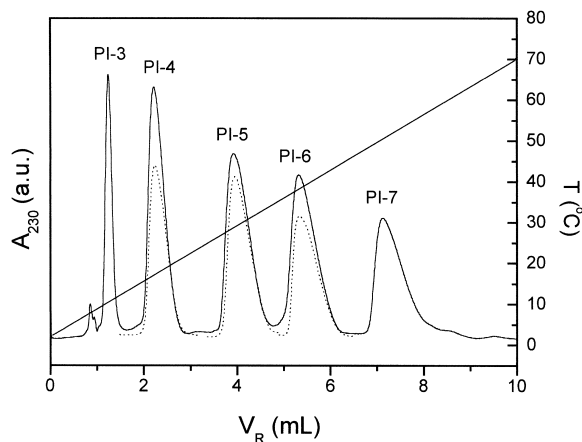


Fig. 1. NP-TGIC chromatogram of a mixture of five PI samples mixture (solid line, from left,  $M_w$ : 20.0, 53.0, 96.0, 148, 208 kg/mol) and individual chromatograms of medium three PI samples (dotted line). Temperature program is also shown in the figure. [Column: diol bonded silica, Nucleosil, 250 mm $\times$ 2.1 mm I.D., eluent: isooctane–THF (98.5:1.5, v/v), flow-rate: 0.1 ml/min].

determined by NP-TGIC are in good agreement with SEC characterization results. On the other hand,  $M_w/M_n$  values calculated from the NP-TGIC analysis are much smaller than those from SEC analysis. These values are quite similar with the results of the RP-TGIC analysis indicating that the resolution of NP-TGIC is comparable to that of RP-TGIC [22]. In accordance with the anionic polymerization theory of Flory, the  $M_w/M_n$  value gets smaller as the molecular mass of PI increases [40]. One important feature in the NP-TGIC relative to RP-TGIC is that both isooctane and THF are good solvents for PI. Therefore we do not have any solubility problem at all for the temperature range of the NP-TGIC analysis. This clearly rules out the possibility of the precipitation–redissolution mechanism [12,41,42] and confirms that the separation mechanism of TGIC is the adsorption interaction.

### 3.2. Fractionation of PS

In order to adjust the adsorption strength of PS with the polar stationary phase, therefore to obtain a good TGIC separation condition for PS, 45% of THF was mixed with isooctane since PS has more polarizable phenyl groups. In this case, bare silica stationary

phase showed a resolution and a reproducibility as good as diol bonded silica. Fig. 2a shows the NP-TGIC separation of a seven PS standard mixture along with individual TGIC runs of five medium-molecular-mass samples. In this case, again peak positions of seven PS samples were fitted by a third-order polynomial function to obtain a calibration curve and MWD was calculated as summarized in Table 2. For a direct comparison with RP-TGIC, the same set of PS samples was investigated by RP-TGIC as shown in Fig. 2b, and MWD of five PS samples were calculated in the same way as in the NP-TGIC case. For the RP-TGIC experi-

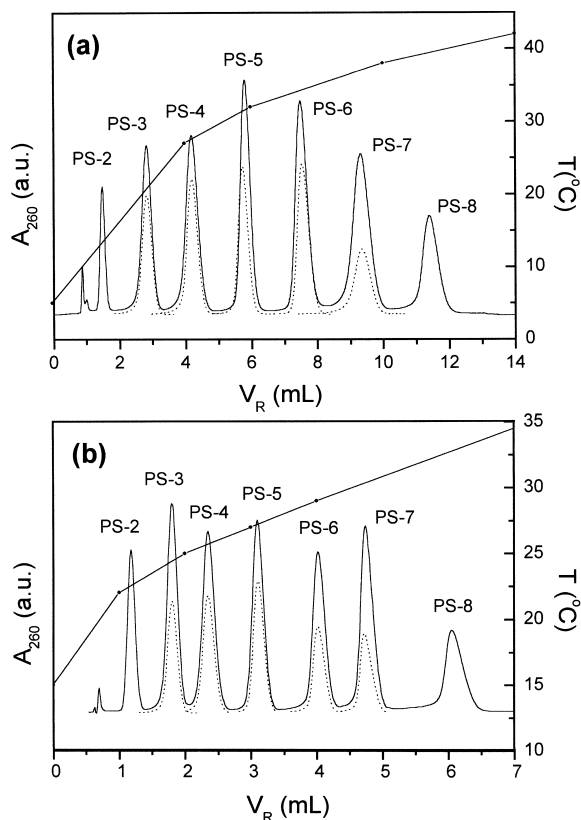


Fig. 2. TGIC chromatograms of a mixture of seven PS samples (solid line, from left,  $M_w$ : 32.7, 68.1, 112, 213, 394, 683, 1530 kg/mol) along with individual run of three PSs for MWD analysis. (a) NP-TGIC [column: silica, Nucleosil, 250 mm $\times$ 2.1 mm I.D., eluent: isooctane–THF (55:45, v/v)], (b) RP-TGIC [column: C<sub>18</sub> bonded silica, Nucleosil, 250 mm $\times$ 2.1 mm I.D., eluent: CH<sub>2</sub>Cl<sub>2</sub>–CH<sub>3</sub>CN (57:43, v/v)]. Flow-rates are 0.1 ml/min and the temperature program for each TGIC run is also shown in the plot.

Table 2  
Molecular mass characterization of polystyrenes by NP and RP-TGIC

Sample code	$M_w (\cdot 10^3)$		$M_w/M_n$	
	NP-TGIC	RP-TGIC	NP-TGIC	RP-TGIC
PS-3	68.1	68.5	1.006	1.008
PS-4	112.3	113.0	1.005	1.006
PS-5	205.7	200.3	1.004	1.004
PS-6	395.5	385.4	1.003	1.004
PS-7	653.4	648.3	1.006	1.006

ments of PS,  $\text{CH}_2\text{Cl}_2$ – $\text{CH}_3\text{CN}$  (57:43, v/v) mixture and a reversed-phase column (Alltech, Nucleosil  $\text{C}_{18}$ , 250 mm  $\times$  2.1 mm I.D.) were used as the mobile and the stationary phase, respectively. The temperature gradient program is also shown in Fig. 2b. The results are summarized in Table 2 and the results from both methods well agree not only in the average molecular mass but also in the MWD.

Although TGIC allows us an extremely high resolution analysis for the MWD characterization of polymers and it is proven to be very useful for a precise MWD analysis of the polymers with narrow MWD [21], long analysis time needed for a TGIC run (1–2 h in Fig. 2) is a clear shortcoming compared to SEC or conventional solvent gradient elution. This is mainly due to the slow heat transfer in a packed column. By employing capillary columns and an improved temperature control design, the analysis time of TGIC could be shortened significantly. At the moment, we are exploiting the merits of TGIC, which are: (1) far better resolution than SEC, (2) more fine and reproducible control of the solute retention than solvent gradient elution HPLC, and (3) more freedom to choose detectors (such as refractive index detector and light scattering detectors) by virtue of using isocratic condition [24].

In both RP and NP methods, the sorption of polymer chains to the stationary phase is an exothermic process since the PS samples are eluted in the sequence of increasing molecular mass when the positive temperature gradient was applied in both NP and RP TGIC experiments. The thermodynamic parameters involved in the RP-TGIC fractionation of PS have been already investigated in the previous paper, in which the enthalpy of adsorption was evaluated from the temperature dependence of the retention [24]. In this study, a similar analysis for

NP-TGIC was performed. Assuming that the adsorption–desorption process is the major retention mechanism of NP-TGIC, the enthalpy of adsorption can be evaluated since the capacity factor ( $k'$ ) has the following relationship with the thermodynamic parameters involved in the separation process:

$$\ln k' = \ln K\Phi = -\Delta H/RT + \Delta S/R + \ln \Phi \quad (1)$$

where  $K$  is the distribution coefficient of a solute between the mobile and stationary phase,  $\Phi$  is the volume ratio of the stationary phase to the mobile phase, and  $\Delta H$  and  $\Delta S$  represent the change of enthalpy and entropy of the solute involved in the adsorption process, respectively. Since we are dealing with the macromolecules that can access to the finite pore volume of the porous stationary phase, the capacity factor could be modified as follows [8]:

$$k' = \frac{V_R - V_{\text{SEC}}}{V_{\text{SEC}}} \quad (2)$$

where  $V_R$  is the retention volume of the solute and  $V_{\text{SEC}}$  is the retention volume of the same solute in a non-adsorbing condition. With the same mobile and stationary phase condition for NP-TGIC of PS as shown in Fig. 2a, van 't Hoff plots were made within the temperature range of 3–44°C using seven PS samples. In order to improve the accuracy of the measurement, three values of  $V_R$  after consecutive injections were averaged and plotted with the standard deviation.  $V_{\text{SEC}}$  of each PS was measured using pure THF as a mobile phase. As shown in Fig. 3, a linear relationship of  $\ln k'$  vs.  $1/T$  was obtained for every PS sample of different molecular mass. From the slope of the van 't Hoff plot, the enthalpy of adsorption,  $\Delta H$  for each PS sample was determined and plotted as a function of the molecular mass in

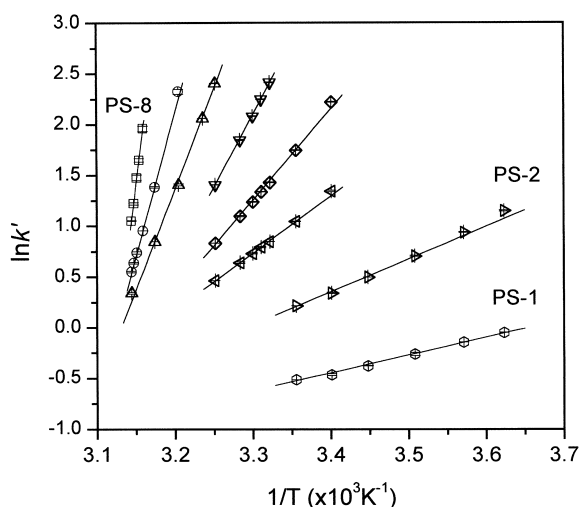


Fig. 3. van 't Hoff plots of eight PS samples (from bottom,  $M_w$ : 10.3, 32.7, 68.1, 112, 213, 394, 683, 1530 kg/mol) under the stationary and mobile phase conditions of Fig. 2a.

Fig. 4a. In Fig. 4b the apparent capacity factors of eight PS samples at 20°C calculated according to Eq. (1) are displayed.  $\Delta H$  and  $\Delta S/R + \ln \Phi$  values were obtained from the slope and the intercept of the van 't Hoff plots in Fig. 4a, respectively. It is clear that  $\Delta H$  is negative for the solute adsorption to the stationary phase and the magnitude of  $\Delta H$  increases with the molecular mass of PS. However, the relationship of  $\Delta H$  vs.  $M$  is not completely linear. Initially, the slope ( $=d\Delta H/dM$ ) at the low-molecular-mass region shows the enthalpy of adsorption is approximately 80 J/mol per monomer unit, which is comparable to that of the RP case [24]. However it decreases down to the value less than 50 J/mol per monomer unit beyond the molecular mass over  $2.0 \cdot 10^4$  g/mol. Similar deviation from linearity is also observed for  $k'$  in Fig. 4b.

According to the Martin's rule, the adsorption energy of a polymeric solute consists of additive contributions of the individual segments of repeat unit [43]. If the Martin's rule holds,  $\ln k'$  vs.  $M$  is supposed to be linear.

Such deviations from the Martin's rule similar to our observation have been reported earlier with somewhat different interpretations [8,33,44]. Larman et al. proposed that the collapse of the extended configuration of high-molecular-mass polymer

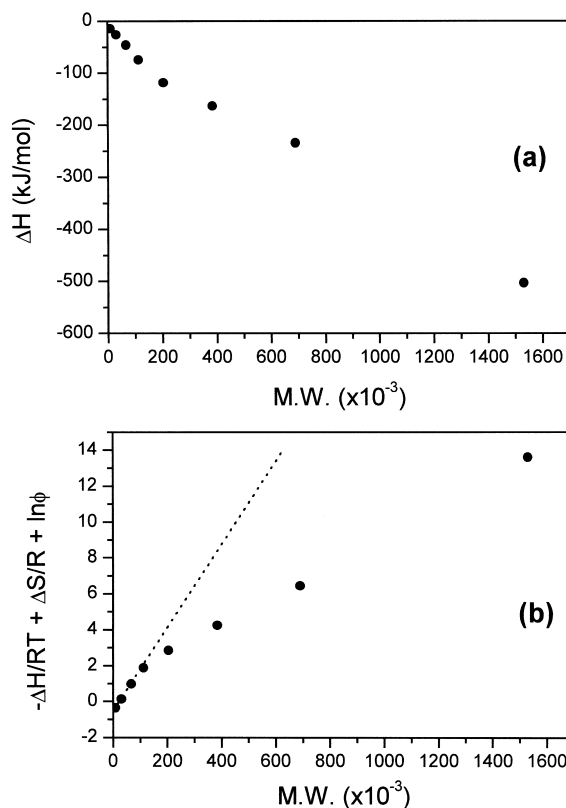


Fig. 4. Plot of the thermodynamic parameters obtained from the van 't Hoff analysis of PS in Fig. 3. (a)  $\Delta H$  vs. molecular mass, (b)  $-\Delta H/RT + \Delta S/R + \ln \Phi$  ( $= \ln k'$ ) calculated at 20°C vs. molecular mass where the deviation from the Martin's rule is shown.

chains might be responsible for the bending of the Martin plot in their RPLC analysis of PS [8]. Jandera and Rozkošná have also found that PS oligomer showed a similar phenomenon in a silica column and it was attributed to non-equal contributions of repeat unit to the energy of adsorption as the molecular mass of polymer increases [33]. More recently, Philipsen et al. discussed the curvature of Martin plot in RPLC with  $C_{18}$  stationary phase using oligomeric PS and polyester as solutes. They ascribed the origin of the curvature to a change of interaction mechanism from "partition" to "sorption" since  $C_{18}$  bonded phase has finite layer thickness for oligomeric species to be fully soaked, while high polymer with larger dimension can access only limited  $C_{18}$  layer [44]. None of the explanations seems to be

fully satisfactory for our observation considering our use of bare silica and high-molecular-mass PS. We think that we have to consider two other factors. One is the possibility of the temperature dependence of the THF adsorption on silica surface. In Fig. 3 we can note that the temperature range in which the van 't Hoff plot was obtained were different for each molecular mass PS sample. If the amounts of THF adsorbed on silica surface changes with temperature, it would have affected the silica surface character to result in the deviation from the Martin's rule. The other factor to be considered is the pore size of the stationary phase. Since the high-molecular-mass polymer chains are excluded from the pore, we used Eq. (2) to calculate the capacity factors. The  $V_{SEC}$  was measured under a good solvent condition (THF), but it would not represent the chain dimension of the PS samples under NP-TGIC conditions satisfactorily. Recently, Baran et al. reported that with the mixture of THF–hexane, the gyration radii of PS ( $M_w = 1.2 \cdot 10^6$  g/mol) decreases from 62 to 45 nm when hexane contents were varied from 0 to 55% which cover the regime of a good solvent and theta solvent for PS [36]. The situation is probably similar in our case since both hexane and isooctane are typical nonpolar solvents for NP-HPLC. Further investigation on the nature of the apparent deviation from the Martin's rule is in progress and will be reported later.

### 3.3. Sensitivity of NP-TGIC to polar end groups

A special feature of NPLC is the sensitivity to polar groups. In order to test the sensitivity of NP-TGIC to polar groups, separation of two PS pairs having identical molecular mass, but different end groups was carried out. Two different molecular mass PS samples ( $M_w = 1.1 \cdot 10^4$  and  $1.05 \cdot 10^5$  g/mol) were prepared by typical anionic polymerization method under an Ar atmosphere using cyclohexane and 2-butyl lithium as solvent and initiator, respectively [37]. After the monomer is completely consumed, a part of the living PS anion was made to react with ethylene oxide to attach a hydroxyl end group while the other portion was directly terminated with methanol. SEC characterization revealed that the PS pairs with different end groups are indistinguishable. A mixture of the two sets ( $1.1 \cdot 10^4$  and

$1.05 \cdot 10^5$  g/mol) of PS (H terminated) and PS-OH (OH terminated) was subjected to NP- and RP-TGIC analysis, respectively. Fig. 5a displays a NP-TGIC chromatogram in which every four PS samples were fully resolved by a single TGIC run while RP-TGIC could separate them only by molecular mass and not by the end group difference at all as shown in Fig. 5b. It is indeed remarkable that NP-TGIC could fully resolve PS and PS-OH of  $1.05 \cdot 10^5$  g/mol molecular mass by a single OH group difference. To our knowledge, there are few other analytical tools available to distinguish such a subtle difference in a long polymer chain.

Another example of such high selectivity is shown in Fig. 6 where NP- (Fig. 6a) and RP- (Fig. 6b) TGIC chromatograms of star shaped PS samples are compared side by side. Ten chromatograms shown in each figure are for the aliquots taken at 10 different

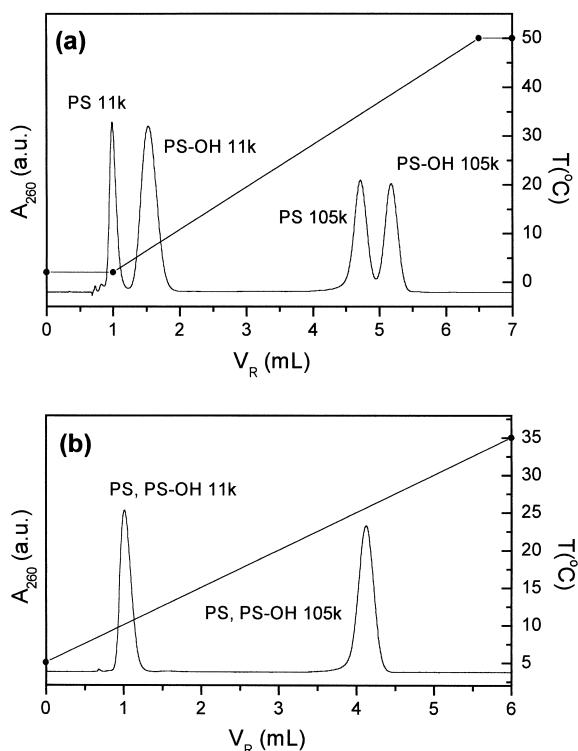


Fig. 5. TGIC separation of PS samples with different end groups (hydrogen terminated vs. hydroxyl terminated) by (a) NP-TGIC and (b) RP-TGIC. Temperature programs are also drawn in each figure. Experimental conditions as described in Fig. 2 except for the temperature program.

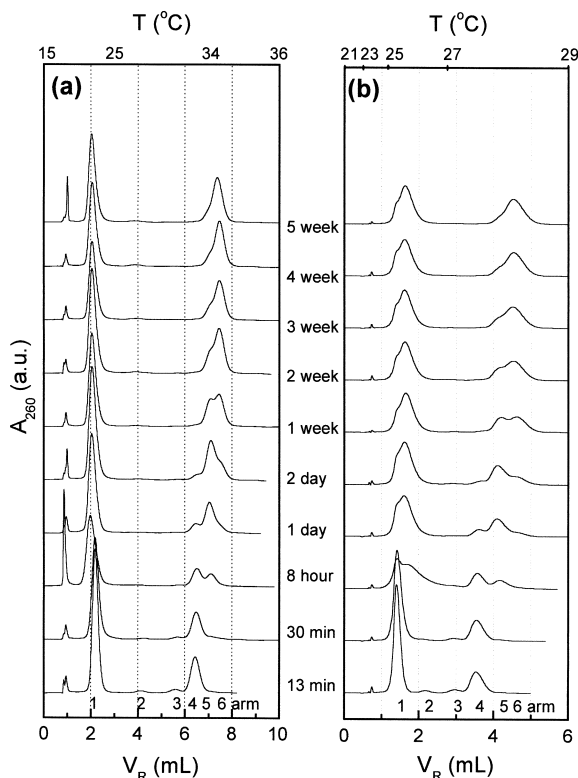


Fig. 6. TGIC chromatograms of 10 star PS samples ( $M_w$  of PS arm:  $8.0 \cdot 10^4$  g/mol) taken from the reactor at various linking reaction times. (a) NP-TGIC (experimental set-up as that of Fig. 2a), (b) RP-TGIC (experimental set-up as that of Fig. 2b). Temperature programs for each case are also shown on the top axis.

reaction times during a linking reaction of living anionic PS precursors with a hexavalent chlorosilane compound [45]. The chromatograms show that star PS with more number of arms is progressively formed as the reaction proceeds and a large amount of unlinked arm remains due to the use of excess amount of the arm materials. Detailed discussion of the linking kinetics of the star PS formation was reported previously [18]. One unresolved question in the RP-TGIC analysis was the appearance of the broadened peak of the unlinked arm after 8 h [18]. By light scattering detection, it was confirmed that all the unlinked arm peaks of the 10 different samples have the identical molecular mass in spite of the broadened peak shape [24]. We speculated that the peak broadening was likely to be caused from

unknown side reactions during the splitting process of the aliquot at 8 h of reaction time. But we could not identify the nature of the side reaction by simple analytical tools such IR or NMR spectroscopy due to the subtle chemical difference and the high-molecular-mass of the precursor PS ( $8 \cdot 10^4$  g/mol) [18]. When we subjected the star PS samples to NP-TGIC, the elution peak shape of the unlinked arms changes significantly while other features of the chromatogram remain almost unchanged. Compared to the RP-TGIC results in Fig. 6b, NP-TGIC shows less broadening of the precursor peaks, and interestingly, the broadening took place in the opposite direction (most clearly visible for the sample taken at 8 h reaction time). This tells us that a part of the precursor arms became less polar due to the side reaction. However, the nature of the side reaction still remains unidentified because the concentration of the end group in the polymer chain is too low to be characterized by simple analytical methods.

### 3.4. Simultaneous SEC–TGIC fractionation of PS and PI mixtures

The other interesting application of NP-TGIC is the simultaneous SEC–TGIC separation of PI and PS mixtures. In the previous paper, we reported simultaneous fractionation of PS and PI by RP-TGIC [22]. In the RP-TGIC system, PS was fractionated in the SEC regime while PI was fractionated in IC regime if we employed the TGIC separation condition for PI since the mobile phase at the separation condition is a good solvent for PS. In the NP system, the separation mechanisms for the two polymer species are reversed since the mobile phase of THF–isooctane (45:55), the NP-TGIC condition for PS, is a good solvent for PI. As displayed in the chromatogram shown in Fig. 7a, five PI samples with different molecular mass are separated by SEC mechanism before the solvent elution peak appears near  $V_R = 11$  ml while eight PS samples are separated by IC mechanism after the solvent peak is eluted. In order to improve the resolution of the SEC separation, three silica columns having different pore sizes (1000, 500, 100 Å, respectively) were connected to obtain the chromatogram. For easy comparison of the separation efficiencies of SEC and TGIC, a



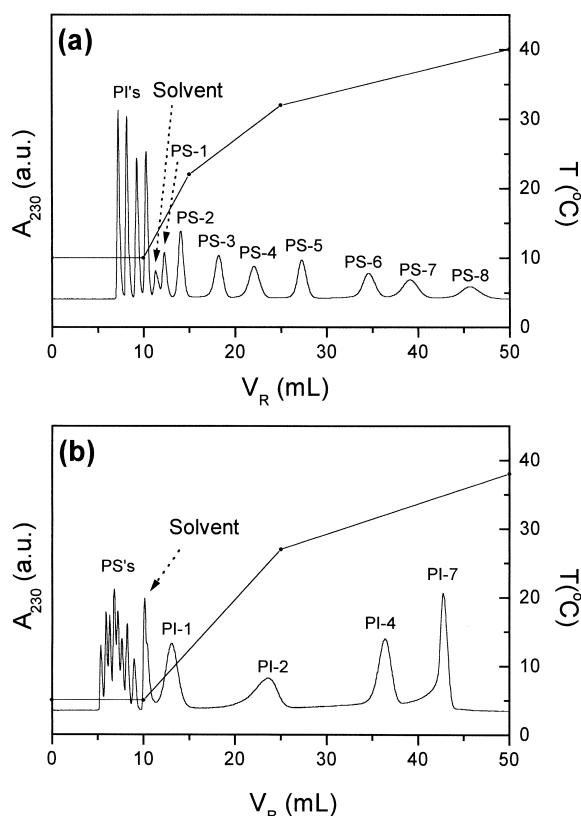


Fig. 7. Simultaneous SEC–TGIC chromatograms of a PI–PS mixture. (a) NP–TGIC chromatogram. PIs (from left,  $M_w$ : 2.7, 11.9, 53.0, 208 kg/mol) are separated by SEC mode while PSs (from left,  $M_w$ : 10.3, 32.7, 68.1, 112, 213, 394, 683, 1530 kg/mol) are separated by TGIC mode. [Column: three bare silica columns having different pore sizes (1000, 500, 100 Å), Nucleosil, 250 mm  $\times$  4.6 mm I.D., eluent: isooctane–THF (55:45, v/v), flow-rate: 0.5 ml/min]. (b) RP–TGIC chromatogram. Elution order is reversed since PI is favorably adsorbed compared to PS in RP mode. [Column:  $C_{18}$  bonded silica columns having different pore sizes (1000, 500, 100 Å), Nucleosil, 250 mm  $\times$  4.6 mm I.D., eluent:  $\text{CH}_2\text{Cl}_2$ – $\text{CH}_3\text{CN}$  (80:20, v/v), flow-rate: 0.5 ml/min].

simultaneous separation of the same sample sets using an RP system was also performed: three Nucleosil  $C_{18}$  columns of different pore sizes (1000, 500, and 100 Å) and a  $\text{CH}_2\text{Cl}_2$ – $\text{CH}_3\text{CN}$  (80:20, v/v) mixture were used as the stationary and the mobile phase, respectively. The RP–TGIC chromatogram is shown in Fig. 7b. It is clear that the elution sequence is completely reversed in molecular mass as well as in polymer species, and the well-resolved TGIC separation of PS samples under NP condition is

much deteriorated when separated by SEC mechanism under RP conditions.

In summary, NP–TGIC analysis of PI and PS was investigated using isooctane–THF mixture as a mobile phase. The resolution of NP–TGIC analysis of PI and PS including star shaped PS was as good as that of RP–TGIC. From the temperature dependence of the capacity factor, it was found that the adsorption of PS on the NP stationary phase was exothermic. NP–TGIC has an advantage over RP–TGIC as exemplified in the investigation of the polymers with polar end group. Furthermore, simultaneous SEC and TGIC analysis of PI–PS mixtures was possible and as expected, the separation mode was reversed relative to the RP system.

### Acknowledgements

This work is supported by the Korea Research Foundation through the Polymer Research Institute of POSTECH and the BK21 program. We also acknowledge the support of POSTECH for the HPLC instrument and Professor Jimmy Mays at the University of Alabama, AL, USA, for the star shaped PS samples.

### References

- [1] W.W. Yau, J.J. Kirkland, D.D. Bly, *Modern Size-Exclusion Liquid Chromatography, Practice of Gel Permeation and Gel Filtration Chromatography*, Wiley, New York, 1979.
- [2] L.R. Snyder, J.J. Kirkland, *Introduction to Modern Liquid Chromatography*, Wiley–Interscience, New York, 1979.
- [3] S.T. Balke, *Characterization of Complex Polymers by Size Exclusion Chromatography and High Performance Liquid Chromatography*, Wiley, New York, 1991.
- [4] A.F. Johnson, M.A. Mohsin, Z.G. Meszena, J. *Macromol. Sci. Rev. Macromol. Chem. Phys.* C39 (1999) 527.
- [5] A. Alhedai, R.E. Boehm, D.E. Martire, *Chromatographia* 29 (1990) 313.
- [6] D.W. Armstrong, K.H. Bui, *Anal. Chem.* 54 (1982) 706.
- [7] R.E. Boehm, D.E. Martire, D.W. Armstrong, K.H. Bui, *Macromolecules* 16 (1983) 466.
- [8] J.P. Larmann, J.J. Destefano, A.P. Goldberg, R.W. Stout, L.R. Snyder, M.A. Stadalius, *J. Chromatogr.* 255 (1983) 163.
- [9] C.H. Lochmüller, C. Jiang, M. Elomaa, *J. Chromatogr. Sci.* 33 (1995) 561.
- [10] C.H. Lochmüller, C. Jiang, Q.C. Liu, V. Antonucci, M. Elomaa, *Crit. Rev. Anal. Chem.* 26 (1996) 29.

- [11] D.M. Northrop, D.E. Martire, R.P.W. Scott, *Anal. Chem.* 64 (1992) 16.
- [12] M.A. Quarry, M.A. Stadalius, T.H. Mourey, L.R. Snyder, *J. Chromatogr.* 358 (1986) 1.
- [13] R.A. Shalliker, P.E. Kavanagh, I.M. Russell, *J. Chromatogr.* 558 (1991) 440.
- [14] R.A. Shalliker, P.E. Kavanagh, I.M. Russell, D.G. Hawthorne, *Chromatographia* 33 (1992) 427.
- [15] R.A. Shalliker, P.E. Kavanagh, I.M. Russell, *J. Chromatogr. A* 679 (1994) 105.
- [16] L.R. Snyder, M.A. Stadalius, M.A. Quarry, *Anal. Chem.* 55 (1983) 1413A.
- [17] H.C. Lee, T. Chang, *Polymer* 37 (1996) 5747.
- [18] H.C. Lee, W. Lee, T. Chang, J.S. Yoon, D.J. Frater, J.W. Mays, *Macromolecules* 31 (1998) 4114.
- [19] H.C. Lee, T. Chang, S. Harville, J.W. Mays, *Macromolecules* 31 (1998) 690.
- [20] W. Lee, H.C. Lee, T. Park, T. Chang, J.Y. Chang, *Polymer* 40 (1999) 7227.
- [21] W. Lee, H. Lee, J. Cha, T. Chang, K.J. Hanley, T.P. Lodge, *Macromolecules* 33 (2000) 5111.
- [22] W. Lee, H.C. Lee, T. Park, T. Chang, K.H. Chae, *Macromol. Chem. Phys.* 201 (2000) 320.
- [23] W. Lee, H.C. Lee, T. Chang, S.B. Kim, *Macromolecules* 31 (1998) 344.
- [24] T. Chang, H.C. Lee, W. Lee, S. Park, C. Ko, *Macromol. Chem. Phys.* 200 (1999) 2188.
- [25] H.C. Lee, T. Chang, *Macromolecules* 29 (1996) 7294.
- [26] F. Kamiyama, H. Matsuda, H. Inagaki, *Polym. J.* 1 (1970) 518.
- [27] E.P. Otocka, *Macromolecules* 3 (1970) 691.
- [28] B.G. Belenkii, E.S. Gankina, M.B. Tennikov, L.Z. Vilenchik, *J. Chromatogr.* 147 (1978) 99.
- [29] P. Holt Sackett, R.W. Hanah, W. Slavin, *Chromatographia* 11 (1978) 634.
- [30] S. Pokorny, J. Janca, L. Mrkvickova, O. Tureckova, J. Trekova, *J. Liq. Chromatogr.* 4 (1981) 1.
- [31] S.T. Lai, D.C. Locke, *J. Chromatogr.* 252 (1982) 325.
- [32] T.H. Mourey, G.A. Smith, L.R. Snyder, *Anal. Chem.* 56 (1984) 1773.
- [33] P. Jandera, J. Rozkošná, *J. Chromatogr.* 362 (1986) 325.
- [34] G. Czichocki, R. Heger, W.A. Goedel, H. Much, *J. Chromatogr. A* 791 (1997) 350.
- [35] S.H. Nguyen, *Chromatographia* 48 (1998) 65.
- [36] K. Baran, S. Laugier, H. Cramail, *Macromol. Chem. Phys.* 200 (1999) 2074.
- [37] K. Kwon, W. Lee, D. Cho, T. Chang, *Korea Polym. J.* 7 (1999) 321.
- [38] E. Katz, R. Dksteen, P. Schoenmakers, N. Miller (Eds.), *Handbook of HPLC*, Marcel Dekker, New York, 1998.
- [39] J.G. Dorsey, W.T. Cooper, *Anal. Chem.* 66 (1994) 857A.
- [40] P.J. Flory, *Principles of Polymer Chemistry*, Cornell, Ithaca, NY, 1953.
- [41] G. Glöckner, *Gradient HPLC of Copolymers and Chromatographic Cross-Fractionation*, Springer Verlag, Berlin, 1992.
- [42] M.A. Stadalius, M.A. Quarry, T.H. Mourey, L.R. Snyder, *J. Chromatogr.* 358 (1986) 17.
- [43] A.J.P. Martin, *Biochem. Soc. Symp.* 3 (1949) 4.
- [44] H.J.A. Philipsen, H.A. Claessens, H. Lind, B. Klumperman, A.L. German, *J. Chromatogr. A* 790 (1997) 101.
- [45] D.J. Frater, J.W. Mays, C. Jackson, S. Sioula, V. Efstradiadis, N. Hadjichristidis, *J. Polym. Sci. Part B: Polym. Phys.* 35 (1997) 587.